proaches the T state of the R-T model of Monod et al. (1965).

Registry No. PFK, 9001-80-3; ATP, 56-65-5; oATP, 54970-91-1.

REFERENCES

Bazaes, S. (1987) in *Chemical Modification of Enzymes—Active site studies* (Eyzaguirre, J., Ed.) pp 35-44, Ellis Horwood Series in Biochemistry and Biotechnology, Chichester, U.K.

Colman, R. F. (1983) *Annu. Rev. Biochem. 52*, 67-91.

Cook, P. F., Rao, G. S. J., Hofer, H. W., & Harris, B. G. (1987) *J. Biol. Chem. 262*, 14063-14067.

Dallachio, F., Negrini, R., Signorini, M., & Rippa, M. (1976) *Biochim. Biophys. Acta 429*, 629-634.

Easterbrook-Smith, S. B., Wallace, J. C., & Keech, D. B. (1976) *Eur. J. Biochem. 62*, 125-130.

Grassetti, D. R., & Murray, J. F. (1967) *Arch. Biochem. Biophys. 119*, 41-49.

Gregory, M. R., & Kaiser, E. T. (1979) *Arch. Biochem. Biophys. 196*, 199-208.

Hofer, H. W. (1970) *Hoppe-Seyler's Z. Physiol. Chem.* **135**, 649-657.

Kemp, R. G. (1969) *Biochemistry 8*, 3162-3168.

King, M. M., & Carlson, G. M. (1981) *Biochemistry 20*, 4382-4387.

Latshaw, S. P., Bazaes, S., Randolph, A., Poorman, A., Heinrikson, R. L., & Kemp, R. G. (1987) *J. Biol. Chem. 262*, 16072-16077.

Lowe, P. N., & Beechey, R. B. (1982) *Biochemistry 21*, 4073-4082.

Monod, J., Wyman, J., & Changieux, J. P. (1965) *J. Mol. Biol. 12*, 88-118.

Mas, M. T., & Colman, R. F. (1983) *J. Biol. Chem. 258*, 9332-9338.

Payne, M. A., Rao, G. S. J., Harris, B. G., & Cook, P. F. (1991) *J. Biol. Chem. 266*, 8891-8896.

Racker, E. (1947) *J. Biol. Chem. 167*, 843-854.

Rao, G. S. J., Wariso, B. A., Cook, P. F., Hofer, H. W., & Harris, B. G. (1987a) *J. Biol. Chem. 262*, 14068-14073.

Rao, G. S. J., Harris, B. G., & Cook, P. F. (1987b) *J. Biol. Chem. 262*, 14074-14079.

Rao, G. S. J., Cook, P. F., & Harris, B. G. (1991) *J. Biol. Chem. 266*, 8884-8890.

Schwartz, K. J., Nakagawa, Y., & Kaiser, E. T. (1976) *J. Am. Chem. Soc. 97*, 6369-6378.

Schraw, W. P., & Post, R. L. (1989) *Arch. Biochem. Biophys. 269*, 327-338.

Srinivasan, N. G., Rao, G. S. J., & Harris, B. G. (1990) *Mol. Biochem. Parasitol. 38*, 151-158.

Starling, J. A., Allen, B. L., Kaeini, M. R., Payne, D. M., Blytt, H. J., Hofer, H. W., & Harris, B. G. (1982) *J. Biol. Chem. 257*, 3795-3800.

Proton Release during Successive Oxidation Steps of the Photosynthetic Water Oxidation Process: Stoichiometries and pH Dependence†

Fabrice Rappaport* and Jérôme Lavergne

Institut de Biologie Physico-Chimique, 13 rue Pierre et Marie Curie, 75005 Paris, France

Received May 31, 1991; Revised Manuscript Received July 31, 1991

ABSTRACT: Flash-induced absorption changes of pH-indicating dyes were investigated in photosystem II enriched membrane fragments, in order to retrieve the individual contributions to proton release of the successive transitions of the Kok cycle. These stoichiometric coefficients were found to be, in general, noninteger and to vary as a function of pH. Proton release on the $S_0 \rightarrow S_1$ step decreases from 1.75 at pH 5.5 to 1 at pH 8, while, on $S_1 \rightarrow S_2$ the stoichiometry increases from 0 to 0.5 in the same pH range and remains close to 1 for $S_2 \rightarrow S_3$. These findings are analyzed in terms of pK shifts of neighboring amino acid residues caused by electrostatic interactions with the redox centers involved in the two first transitions. The electrochromic shift of a chlorophyll, associated with the S transitions, responding to local electrostatic effects was investigated under similar conditions. The pH dependence of this signal upon the successive transitions was found correlated with the titration of the proton release stoichiometries, expressing the electrostatic balance between the oxidation and deprotonation processes.

An important element for understanding the process of photosynthetic water oxidation is the mechanism of proton release. The overall reaction, $2H_2O \rightarrow O_2 + 4e^- + 4H^+$, involves the abstraction of four electrons which are taken up one at a time by the reaction center of photosystem II (PS II).[1] The oxygen-evolving complex (OEC) thus goes through four successive oxidation states before releasing molecular oxygen. The behavior of the system under illumination by short sat-

† This work was supported by the Centre National de la Recherche Scientifique (U.R.A. 1187).

* Address correspondence to this author.

[1] Abbreviations: PS II, photosystem II; OEC, oxygen-evolving complex; DNP-INT, dinitrophenyl ether of iodonitrothymol; DCBQ, 2,5-dichloro-*p*-benzoquinone; DCMU, 3-(3,4-dichlorophenyl)-1,1-dimethylurea; FCCP, carbonyl cyanide *p*-(trifluoromethoxy)phenylhydrazone; BBY, PS II enriched membrane preparation according to Berthold et al. (1981).

0006-2960/91/0430-10004$02.50/0

urating flashes is classically described by the Kok cycle:

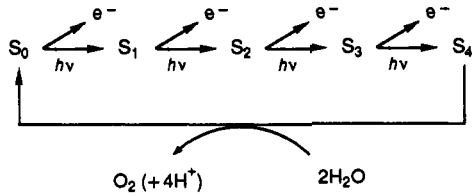

in which state S_4 spontaneously re-reduces toward S_0 in a millisecond reaction accompanying oxygen evolution (Joliot & Kok, 1975). In a pioneering work on proton releasing during the Kok cycle, Fowler (1977a) showed that the protons were not all liberated during the final oxygen-evolving step, nor evenly released upon each step, but obeyed a distinct stoichiometry accompanying each transition of the S states. The larger fraction was observed during the $S_3 \rightarrow S_4 \rightarrow S_0$ (oxygen-evolving) step and the smaller one during $S_1 \rightarrow S_2$. Fowler estimated a stoichiometry close to 1, 0, 1, 2 for the successive transitions. He actually believed the precise pattern to be rather 0.75, 0, 1.25, 2, which he proposed to interpret as a mixture of two integer stoichiometries expressing an heterogeneity in the oxygen-evolving system.

While the proton release steps were first thought to simply express intermediate oxidation reactions of water, it has become clear that the mechanism may be much less direct. It is now broadly accepted that water oxidation most probably proceeds through concerted multielectronic reaction(s) and that at least part of the S transitions correspond to oxidation steps of auxiliary charge-storing redox centers. The key role of a cluster of 4 manganese atoms has been brought to light, and in particular, the $S_1 \rightarrow S_2$ step was shown to correspond to manganese oxidation [see, for reviews, Rutherford (1989) and Babcock (1987)]. Thus, while the final balance of proton release must correspond to the overall water oxidation reaction, the detailed mechanism may involve deprotonation of other species upon intermediate oxidation steps and reprotonation of these species upon the re-reduction step toward S_0.

In the recent years, work by Maroti and Wraight (1988) and McPherson et al. (1988) brought about significant renewal in the perception of protolytic events in reaction centers. These authors analyzed proton release and uptake resulting from charge separation in isolated bacterial centers and showed that proton exchange with the medium was in general obeying noninteger stoichiometries that vary as a function of pH. The interpretation was that the charges appearing on the donor and acceptor sides modify through electrostatic interaction a number of protonation equilibria on neighboring amino acids. It is thus clear that deprotonation reactions in the Kok cycle may involve a wide range of processes, from direct breaking of an O–H bond to deprotonation of an oxidized auxiliary species and to the still more indirect deprotonation of electrostatically influenced amino acid residues.

While Fowler's experiments were performed with a sensitive glass electrode technique, further investigation made use of absorption changes of pH-responding dyes (Saphon & Crofts, 1977; Förster & Junge, 1985). Using an hydrophilic dye that probes the pH of the medium, Saphon and Crofts (1977) further supported the 1, 0, 1, 2 pattern. Similarly to Fowler's approach, the internal acidification was obtained by subtracting the external uptake from the global response (external + internal) measured in the presence of a protonophore. A more direct access to internal events can be obtained by using the amphiphilic dye neutral red that penetrates the lumen and concentrates on the surfaces of the membrane (Ausländer & Junge, 1975). Then, when buffering selectively the external medium, the dye should respond solely to proton exchange in the lumenal space. Combined with the use of an inhibitor (DBMIB or, preferably, DNP-INT) of the other protolytic reaction occurring on the internal side (plastoquinol reoxidation), this method allows sensitive resolution of proton liberation from the oxygen-evolving system. Using this technique, Förster and Junge (1985) also found agreement with the 1, 0, 1, 2 pattern. However, this conclusion was based on the assumption that only the fast phase (terminated in a few milliseconds) of the neutral red response should be taken into account for measuring proton release from PS II. A slower phase of the dye response was observed in the 100-ms range, thus markedly delayed with respect to electron transfer events in PS II, and accordingly believed to express some artifactual response of the dye.

In recent work (Lavergne & Rappaport, 1990), we proposed that the slow phase of the neutral red response was monitoring the transient alkalization of the appressed external regions, which had been shown (Polle & Junge, 1986) to equilibrate with the bulk external medium in the 100-ms range. This transient contribution is indeed expected to occur if BSA, used as a nonpermeating buffer in these experiments, remains excluded from the appressed regions. This reinterpretation of the neutral red responses was extensively tested in collaborative work with Jahns and Junge and was confirmed to be correct (Jahns et al., 1991). This has an important consequence on the determination of proton release stoichiometry in the Kok cycle. Indeed, the lumenal acidification should be estimated from the dye response when the transient external interference is terminated, i.e. taking into account the *total* change rather than the sole slow phase. This results in a less contrasted oscillating pattern in flash sequence experiments, which cannot be accounted by an integer stoichiometry (such as 1, 0, 1, 2) but imposes noninteger figures. As a first approximation, we proposed a 1, $^1/_2$, 1, $^3/_2$ pattern (Lavergne & Rappaport, 1990).

One first goal in the present work has been to cross-check the above conclusions of a noninteger stoichiometry by an independent method free of possible problems arising from the use of whole thylakoids and neutral red. We used PS II enriched membrane fragments ("BBY particles") as a simplified system that has lost the thylakoid vesicular structure and lacks electron transfer toward PS I and quinol reoxidation on the *b–f* complex. Taking advantage of techniques that were developed for deconvolution of absorption changes associated with the S-state transitions in this material (Lavergne, 1991), we have obtained precise determination of the proton release stoichiometry that confirms the qualitative conclusions derived from neutral red experiments. As made clear by the papers of Maroti and Wraight (1988) and McPherson et al. (1988), a noninteger stoichiometry should be expected to be pH-dependent. This was indeed found to be the case and has led us to locate the p*K*'s of some of the groups involved in this process. The combined oxidation and deprotonation reactions affect the electrostatic configuration on PS II donor side and thus modulate an electrochromic shift of a neighboring chlorophyll molecule. We titrated the S-state dependence of this shift as a function of pH and found satisfactory correlation with the proton release data.

Materials and Methods

"BBY particles" were prepared as described by Ghanotakis and Babcock (1983), omitting the second triton incubation. We checked that photooxidation of P-700 was negligible and found no detectable photooxidation of cytochrome *f*. The particles were kept frozen at a 5 mg of chlorophyll/mL con-

centration in a medium containing 0.3 M sucrose, 5 mM $MgCl_2$, 10 mM NaCl, and 2 mM MES, pH 6.2. They were diluted for experimental use at 12.5 μg of chlorophyll/mL in the same medium but containing no MES, nor $MgCl_2$. The pH of the suspension was adjusted as required. Except when indicated otherwise, 20 μM DCBQ and 2 nM FCCP were added. For proton measurements we further added the following dyes: bromocresol purple at pH ≤7 or phenol red at pH ≥7. The dye concentration was in the 20–40 μM range, depending on the pH region investigated.

Absorption changes were measured with the Joliot spectrophotometer (Joliot et al., 1980; Joliot & Joliot, 1984) where the absorption is sampled at discrete times with short monochromatic flashes. Xenon flashes of 2-μs half-width duration, filtered with a broad-band red filter, were used for actinic illumination and cheked to be saturating under all our experimental conditions. Absorption changes of bromocresol purple were monitored at 570 nm, and those of phenol red at 545 nm. The intrinsic signals in the absence of dyes were found negligible at both wavelengths. Further details on the experimental procedure are given in the next section.

Determination of Proton Stoichiometry from Flash Sequence Data. We denote by $S_i(n)$ the amount of state S_i present after flash n, and by α and β the probabilities of, respectively, photochemical misses and double hits. The evolution of $S_i(n)$ is given by the recurrence relation:

$$S_i(n) = \alpha S_i(n-1) + (1-\alpha-\beta)S_{i-1}(n-1) + \beta S_{i-2}(n-1) \quad (1)$$

where the i's are taken modulo 4. Starting from a dark-adapted state (fully deactivated), the only stable states are S_0 and S_1. Denoting by σ the initial amount $S_0(0)$, one has $S_1(0) = 1-\sigma$ and $S_2(0) = S_3(0) = 0$. Thus, according to eq 1, the evolution of the system is entirely determined by three parameters, α, β, and σ. Now, if ϵ_i denotes the stoichiometry of proton liberation on step $S_i \rightarrow S_{i+1}$, the sequence of proton release is

$$\Delta H(n) = \sum_{i=0}^{3} \epsilon_i T_i(n) \quad (2)$$

where $T_i(n)$ denotes the weight of transition $S_i \rightarrow S_{i+1}$ upon flash n. This is given by

$$T_i(n) = (1-\alpha)S_i(n-1) + \beta S_{i-1}(n-1) \quad (3)$$

Since the overall stoichiometry is 4 protons per cycle, one has $\epsilon_3 = 4 - (\epsilon_0 + \epsilon_1 + \epsilon_2)$. Thus eq 2 becomes

$$\Delta H(n) = \epsilon_0[T_0(n) - T_3(n)] + \epsilon_1[T_1(n) - T_3(n)] + \epsilon_2[T_2(n) - T_3(n)] + 4T_3(n) \quad (4)$$

This is a linear system with three unknowns (ϵ_0, ϵ_1, and ϵ_2), in which $\Delta H(n)$ is obtained from experiment and the T's are computed from eqs 1 and 3, knowing α, β, and σ. Three equations (flashes) are strictly required to solve the system, while using a longer sequence and an appropriate least-squares procedure (Lavergne, 1987) will improve the resolution. The absorption change on the first flash was excluded from the computation, since it contains an extraneous contribution (with respect to the Kok cycle), as previously discussed (Dekker et al., 1984; Lavergne, 1987, 1991).

In most practical cases, the flash sequence data may contain additional signals, e.g., from the acceptor side. If one can manage to make these signals constant upon each flash, this amounts to an offset in the sequence that may easily be dealt with by introducing a corresponding fourth unknown (steady-state level) when solving the system.

Computation of the ϵ's from eq 4 implies prior determination of the Kok parameters α, β, and σ. This problem was extensively discussed in previous work (Lavergne, 1991), and the same methods were used here. In order to determine α and β, we used Lavorel's equation (Lavorel, 1978) on the sequence of (14) flashes associated with the S transitions at 290 nm. This method may be applied to any S-dependent sequence and could be used directly on the proton sequence. However, the UV sequence is more contrasted and allows a better resolution. Furthermore, the measurement of this sequence at each pH provides a valuable check on the functioning of the Kok cycle. In order to determine σ (initial S_0/S_1 distribution), the system was preilluminated by one flash and allowed to fully deactivate in the dark before running the experiment. Since state S_2 deactivates toward S_1, this procedure sets the system to almost 100% S_1 (97–99%) with rather weak dependence on the initial dark-adapted state. In order to accelerate somewhat the deactivation rate, we added a low (2 nM) concentration of FCCP, which allows complete deactivation in less than 4 min [as shown by Lavergne (1991), no effect of this addition on the sequences was otherwise detectable]. In order to make sure of the validity of this procedure under all the pH conditions involved in this study, we systematically checked that the σ obtained through the one-preflash procedure was indeed close to zero by using the difference method (on 290-nm sequences) described by Lavergne (1991). In this case, the deconvolution is computed from the difference of two sequences (using, e.g., one and three preillumination flashes) and allows *experimental determination* of the σ's.

In order to obtain the $\Delta H(n)$ data, one has to eliminate or subtract the possible proton uptake on the acceptor side. In principle, the simpler way to do so should be using ferricyanide as an acceptor. Since this compound does not protonate upon reduction, the pH changes should directly express proton release by the Kok cycle. However, several difficulties are encountered when using ferricyanide. First, the UV checks described above become impossible because of the absorbance of ferricyanide in this region, precluding an accurate determination of the Kok parameters under the same conditions as when recording the dye absorption changes. Second, the addition of ferricyanide is known to cause oxidation of the non-heme iron on the acceptor side of PS II, particularly at high pH, which is expected to result in an increased fraction of double hits on the first flash (Petrouleas & Diner, 1986). Since the extent of this phenomenon is difficult to estimate accurately, the deconvolution of the ϵ's would become very unreliable. Third, the kinetics of the dye response in the presence of ferricyanide were found to include a slow phase in the seconds time range, suggesting a heterogeneity in the accessibility to ferricyanide and complicating the interpretation of the data. For these reasons, we prefered recording the proton sequence in the presence of DCBQ (20 μM) as an electron acceptor, using ferricyanide only in a final step aimed at calibrating the dye response. A possible problem when using a quinonic acceptor would be a flash-dependent uptake correlated with the binary variation of the semiquinone bound in the Q_B pocket. Actually, such a binary flash dependence of the uptake does not occur with the endogenous plastoquinone (Fowler, 1977b) for which both reduction steps of Q_B cause the uptake of one proton. However, this may not hold at any pH, or when using DCBQ. We could, however, exclude this possibility by using two sorts of tests. First, when running the difference method outlined above on a set of two (one or three preflash) absorption change sequences of the dye, we

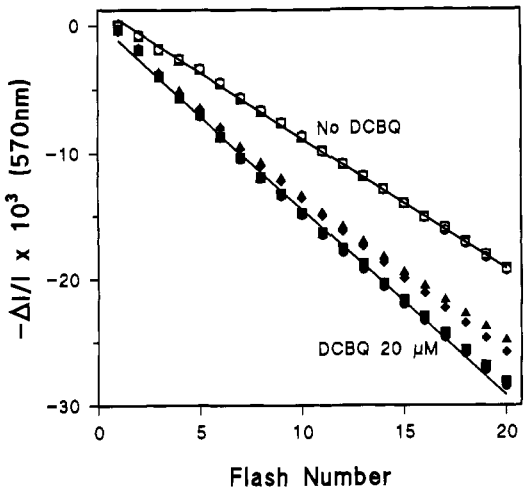

FIGURE 1: Absorption changes of bromocresol purple during a series of 20 flashes spaced 1 s apart with various concentrations of ferricyanide (triangles, 5 μM; squares, 100 μM; circles, 200 μM; diamonds, 2 mM) in the presence (solid symbols) or absence (open symbols) of 20 μM DCBQ. The pH was 6.5 and the dye concentration 25 μM. The solid lines show the linear regression of the data with 100 μM ferricyanide.

obtained, at each pH, essentially similar results to those derived from a single sequence (one preflash, assuming $\sigma \approx 0.02$). Since non-S contribution should cancel in the difference, the agreement between both methods warrants the absence of a significant binary perturbation in the one-preflash sequence. A second test was to increase the DCBQ concentration to 150 μM. Under such conditions, total reoxidation of the semiquinone formed upon each flash occurs in a few hundred ms, thus eliminating binary semiquinone oscillations at a flashing frequency of 1 Hz (Lavergne, 1991). There again, the results were essentially identical with those obtained at lower DCBQ concentration. The reason for using 20 μM DCBQ in routine experiments was a decreased lifetime of the sample activity at higher concentrations. We thus conclude that, under the conditions we used, electron transfer to DCBQ is accompanied by a constant proton uptake upon each flash.

In order to subtract the constant offset due to proton uptake, one needs a calibration of the dye response in terms of absorption change per proton released per center. This may be obtained in a simple way by measuring the steady-state flash-induced absorption change in the presence of ferricyanide (Fowler & Kok, 1976), which should correspond to one proton per electron transfered to this acceptor. Figure 1 shows the absorption changes of the dye during a train of 20 flashes with various concentrations of ferricyanide, in the presence or absence of DCBQ. As may be seen, the presence of DCBQ increases the rate of the steady-state acidification, suggesting that it mediates efficiently electron transfer toward ferricyanide. No further increase was found at higher DCBQ concentration. When varying the ferricyanide concentration, the maximal slope was obtained above 50 μM, while at higher concentrations ($\geq$2 mM) a slight decrease of the rate was observed, suggesting an inhibitory effect in this range. From these results we conclude that in the presence of 20 μM DCBQ and 200 μM ferricyanide, the steady-state regime corresponds to total electron transfer toward ferricyanide as a terminal acceptor. The acidification slope gives the dye response per flash that corresponds to $[1 - (\alpha + \beta) + 2\beta] = (1 - \alpha + \beta)$ electrons per center, from which we obtain the required calibration. Further details are given in the next section.

We can now summarize our routine procedure. First, the 290-nm sequence was recorded in the presence of 20 μM DCBQ and 2 nM FCCP (one preflash, 4-min deactivation). The dye was then added (pH readjusted) and its absorption change sequence (545 or 570 nm) recorded (one preflash, 4-min deactivation). Finally, 200 μM ferricyanide was added (pH readjusted) and a 15-flash sequence (no preillumination) recorded. The overall duration of the experiment was maintained as short as possible in order to avoid significant drift in the sample activity. The deconvolution results from three or more such experiments were averaged at each pH to obtain the data shown in Figure 4 (in addition to the controls described above using the difference method either on the 290-nm or dye sequences).

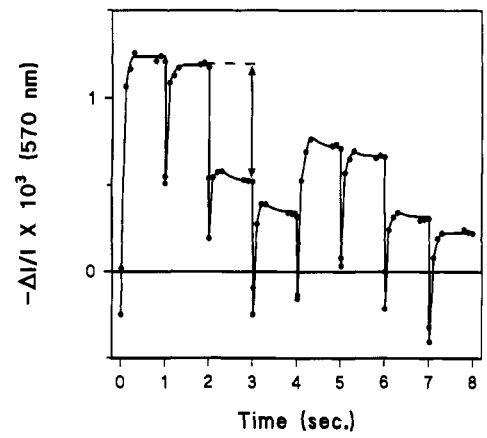

FIGURE 2: Absorption changes of bromocresol purple during a series of flashes spaced 1 s apart. The signal was monitored at discrete times (5, 10, 100, 200, 300, 800, 900, 1000 ms) after each flash. The pH was 6.5 and the dye concentration 25 μM. A downward directed signal corresponds to an acidification. The overall change caused by each flash was obtained as shown by the arrow for the third flash.

Results

pH Dependence of the Proton Release Stoichiometry. Figure 2 shows typical raw data for the absorption changes of bromocresol purple at pH 6.5. The dots indicate the signal sampling at discrete times after each flash. The acidification response (directed downward) is faster than the uptake and is slowed down on the third and seventh flashes, expressing the millisecond reaction accompanying oxygen release. Unfortunately, the kinetic discrimination between the release and uptake is not sharp enough to allow a direct measurement of both contributions. As may be noticed, rapid proton release is observed on all flashes (including the first one), suggesting that this process occurs, to a variable extent, on all S transitions, including $S_1 \rightarrow S_2$. A similar conclusion was drawn from neutral red experiments (Lavergne & Rappaport, 1990; Jahns et al., 1991). In the following, we shall ignore the kinetic aspects and focus on the overall change caused by each flash, measured as indicated by the arrow for the third flash in Figure 2.

Figure 3 illustrates the dye absorption change sequences measured at various pH's. The steady-state level in the latter sequences (indicated as a dashed line) is close to the zero of the absorption change scale (indicated at left) at pH 5.5, but becomes negative at higher pH's. The zero value expresses compensation between the one proton per electron released on the average by the OEC and an identical uptake on the acceptor side. At alkaline pH, the acidification prevails, suggesting an uncomplete protonation of reduced DCBQ. The possibility of an offset of the dye response not associated with pH changes (e.g., electron transfer to the dye) was ruled out by checking the total cancellation of the absorption changes upon addition of a buffer poised at the same pH. From the

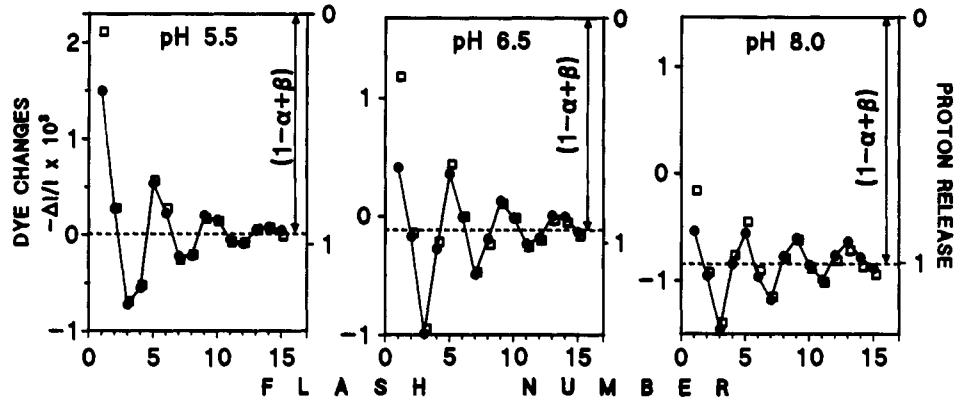

FIGURE 3: Absorption change sequences of the dye at various pH's. Parameters α and β were computed from the S-dependent sequences at 290 nm measured under identical conditions (except no dye was present). The values were respectively the following: 0.13 and 0.09 at pH 5.5; 0.12 and 0.07 at pH 6.5; and 0.06 and 0.07 at pH 8. The dye absorption changes were recorded at 570 nm when using bromocresol purple (40 μM at pH 5.5 and 25 μM at pH 6.5) or at 545 nm when using phenol red (20 μM at pH 8). The dashed lines show the steady-state levels obtained from sequence deconvolution, and the vertical arrows correspond to the acidification signal per flash in the presence of ferricyanide (see Figure 1). The arrow thus gives at each pH the origin of the proton release signal. Since its amplitude corresponds to $(1 - \alpha + \beta)$ proton per center, we computed the proton unit shown on the right-hand scale of each box, using the α, β values given above. Data points are presented as solid circles while the open squares are computed values obtained from deconvolution of the sequences (first flash excluded). The deconvoluted values of the stoichiometric coefficients ϵ_0, ϵ_1, and ϵ_2, were respectively the following: 1.7, 0.0, and 1.0 at pH 5.5; 1.2, 0.2, and 0.95 at pH 6.5; and 1.05, 0.55, and 1.0 at pH 8.

additional measurement of the acidification response in the presence of ferricyanide (see Figure 1), we obtained at each pH the signal corresponding to $(1 - \alpha + \beta)$ proton per flash per center. Plotting this value (vertical arrow) above the steady-state level determines the origin for proton release by the OEC (right-hand scale). Parameters α and β determined from the 290-nm sequence allow the final determination of the proton unit indicated on this scale. The sequences with respect to this proton scale provide the basic material used for computing the release stoichiometries upon the successive S transitions.

The stoichiometric coefficients ϵ computed when solving the linear system (eq 4) for the data of Figure 3 are given in the legend. They deviate quite significantly from an integer pattern and depend on pH, as expected from the pH dependence of the data. The open symbols show the computed values for $\Delta H(n)$ using these coefficients. The agreement with the data is quite good, except for the first flash that was not used in the deconvolution treatment. This particular problem will be further examined in the discussion.

Figure 4 shows the pH dependence of the stoichiometric coefficients as obtained from averaging the results of experiments similar to those of Figure 3. A qualitative agreement is found with the behavior previously described for chloroplasts around pH 7, with a minimum release on the $S_1 \rightarrow S_2$ step and a maximum on $S_3 \rightarrow S_0$. However, the novel results here are that the proton release from the OEC never obeys a simple integer pattern and that the stoichiometric coefficients depend quite significantly on the pH of the medium. In previous reports (Lavergne & Rappaport, 1990; Janhs et al., 1991) we already stressed that an integer pattern such as 1, 0, 1, 2 had to be abandoned. Our guess was that a constant offset was mixed to this pattern, resulting in something like $1, {}^1/_2, 1, {}^3/_2$. From the more precise investigation reported here, it turns out that, while the release upon $S_2 \rightarrow S_3$ remains close to 1, a fractional figure is also involved upon $S_0 \rightarrow S_1$ where more than one proton is released for pH <7.5.

Proton Release in the Presence of DCMU. The titration of Figure 4 relies on a somewhat elaborate deconvolution technique for retrieving the individual contributions of the individual S transitions to the proton release sequence. A useful cross-check can be designed that allows determination of proton release on the $S_1 \rightarrow S_2$ step in a much more direct

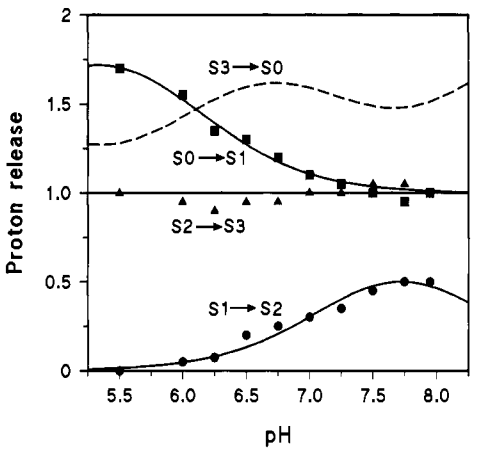

FIGURE 4: pH titration of the stoichiometric coefficients ϵ_0 (squares), ϵ_1 (circles), and ϵ_2 (triangles). The data points were obtained, for each pH, from the averaging of 3–5 experiments similar to those presented in Figure 3. The curves show the fit of the data according to the model described in the text (in the case of $S_1 \rightarrow S_2$, the DCMU data of Figure 5 were also taken into account in the fitting procedure). The $S_3 \rightarrow S_0$ titration (dashed) was computed as the complement to 4 of the sum of the preceding curves.

way. In the presence of DCMU, inhibiting transfer toward the secondary acceptor quinone Q_B, the photoinduced $S_2Q_A^-$ state back-reacts in the dark toward S_1Q_A with a half-time of a few seconds. Centers initially in S_0 will remain blocked in state $S_1Q_A^-$, or possibly may decay on a much slower time scale. Thus, in a regime of light–dark cycles, excluding the first one, the system will shuttle between S_1Q_A and $S_2Q_A^-$. Rather than flash illumination, continuous light can be used, ensuring total charge separation irrespective of the decreased photochemical efficiency occurring at extreme pH's. This point was checked by monitoring independently Q_A reduction through the C-550 absorption change. From measurements with vesicular thylakoids (Polle & Junge, 1986) one knows that no significant proton uptake occurs on Q_A^- in the presence of DCMU. Assuming that this remains true in the whole pH range investigated here, the absorption change of the dye under such conditions should monitor the release accompanying $S_1 \rightarrow S_2$. In order to calibrate the sensitivity of the dye response at various pH's, we measured the absorption change caused by adding known concentrations of protons to the suspension.

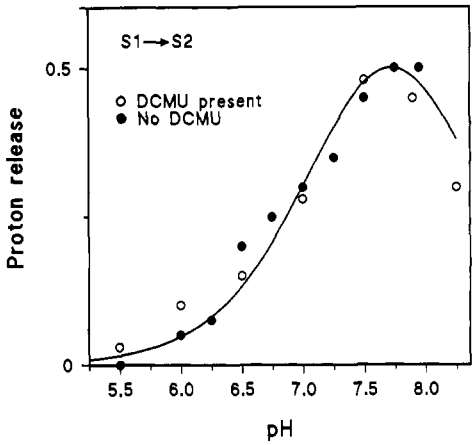

FIGURE 5: Proton release measured in the presence of 2 μM DCMU (closed circles) during a 2-s illumination with continuous light. The sample was submitted to several light (2-s)/dark (60-s) cycles, averaging the signal on all illuminations except the first one. The intensity was adjusted so that the proton release kinetics (or Q_A reduction kinetics) was completed within 200 ms. Identical extent of Q_A reduction as measured through the C-550 change was obtained at each pH under these conditions. Calibration of the proton release scale was achieved by measuring the absorption change of the dye in response to additions of known concentrations of protons to the suspension, assuming the particles contained 250 chlorophylls per PS II center (Berthold et al., 1981). For comparison, we replotted on the same scale (open circles) the $S_1 \rightarrow S_2$ titration data of Figure 4, derived from sequence deconvolution. The solid curve is the best fit for the two sets of data, using the model described in the text (only minor differences of the pK values were obtained when running both fits separately).

The results of this experiment are shown in Figure 5 (closed circles), where the deconvolution data from Figure 4 were also replotted for comparison (open circles). The agreement between both methods is good and confirms the occurrence of a peak around pH 7.75. Nevertheless, some caution may be required as to possible interference of a pH-dependent uptake on Q_A^-.

pH Dependence of the Electrochromic Shift in the Blue Region. Part of the absorption changes associated with the S transitions are known to express local electrochromic effects rather than direct oxidation of a redox carrier. This is clearly the case in the blue and red regions (Dekker et al. 1984; Lavergne, 1987; Saygin & Witt, 1985; Velthuys, 1988) where a shift of a chlorophyll *a* absorption spectrum is observed, mostly on the $S_1 \rightarrow S_2$ step. This signal reflects variations of the electrostatic potential experienced by the probe and should depend on the extent of deprotonation accompanying the S transitions. We thus investigated the S dependence of the shift in the blue region as a function of pH, in order to correlate this electrostatic information with the proton release results. Figure 6, right-hand side, shows the spectra obtained for the successive transitions in this region at pH 6.5 as obtained by Lavergne (1991). The shift observed on $S_1 \rightarrow S_2$ consists of two peaks (415 and 440 nm) and a trough at 430 nm. It is also present with an inverted sign and smaller amplitude on the $S_0 \rightarrow S_1$ step and absent to a significant extent on $S_2 \rightarrow S_3$.

In the left-hand panel of Figure 6, we plotted the amplitude of the shift estimated as the difference 428 nm − 440 nm (trough minus peak) for each S transition as a function of pH. The differential method using two sequences (one and three preillumination flashes) at each of these wavelengths and at 290 nm was applied as previously described (Lavergne, 1991). This procedure was designed to eliminate any possibly remaining binary contribution from the acceptor side. For

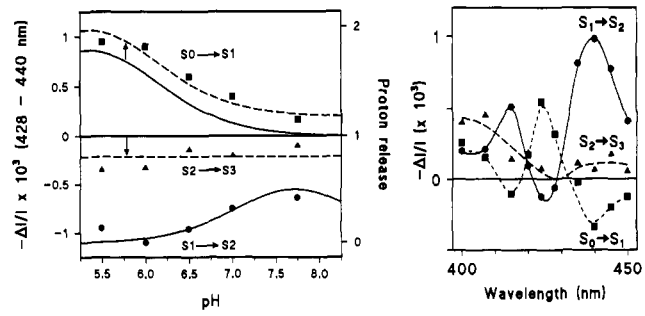

FIGURE 6: Electrochromic shift in the blue region and its pH dependence. The right-hand panel [data from Lavergne (1991)] shows the spectra obtained, at pH 6.5, for the successive transitions. The left-hand panel presents the pH titration of the amplitude of the shift (428-nm trough minus 440-nm peak) on each transition. The solid lines are a replot of the proton release titrations of Figure 4 with arbitrary normalization on the $S_1 \rightarrow S_2$ data point at pH 6.5. A better fit (dashed curves) of the electrochromic data was obtained by shifting the $S_0 \rightarrow S_1$ and $S_2 \rightarrow S_3$ curves by an offset indicated by the vertical arrows.

comparison, the proton release dependence was replotted from Figure 4 with an arbitrary normalization on $S_1 \rightarrow S_2$ at pH 6.5. The overall agreement between both pieces of information provides a rather satisfactory cross-check of the present results as a whole.

Discussion

The main result of the present work is a clear contradiction with the broadly accepted 1, 0, 1, 2 pattern for proton release during the Kok cycle. In place of this simple integer stoichiometry, we have found noninteger, pH-dependent values, which modify significantly the perception of mechanisms involved in this process. Before discussing the interpretative aspects, it may be useful to briefly comment on earlier work on the subject. All the classical work (Fowler, 1977a; Saphon & Crofts, 1977, Förster & Junge, 1985) concluding for the 1, 0, 1, 2 model was done with thylakoids. If we leave apart the neutral red experiments (Förster & Junge, 1985) (in which the problem was an unwarranted rejection of the slower response phase of the dye), these experiments had to correct for protolytic events on the *b–f* complex, which considerably complicates the analysis. Besides, the spontaneous approach was to expect an integer stoichiometry, or at most a mixture of two integer stoichiometries (Fowler, 1977a). Indeed, release of fractional protons may have seemed an awkward idea until recent work on bacterial reaction centers (McPherson et al., 1988; Maroti & Wraight, 1988) showed that it did happen and could be actually rather naturally expected from simple electrostatic considerations. We thus believe that the expectation of an integer stoichiometry was a significant bias in earlier reports. The 1, 0, 1, 2 model is indeed the best integer pattern that accounts for the proton release data showing a clear minimum on $S_1 \rightarrow S_2$ and maximum on $S_3 \rightarrow S_0$. Inaccurate estimation of an offset in the sequences or of the signal calibration may easily mislead toward an integer pattern. This was the case in neutral red experiments (Förster & Junge, 1985) (where a constant offset was neglected), but also in Fowler's (1977a) work where the calibration was, under all likelihood, faulty. Indeed, this author reported an overall proton to electron ratio for transfer from water to methyl viologen of 4 whereas this value is now known to be 2 or 3, depending of the efficiency of the Q-cycle process in the *b–f* complex. This calibration error causes a base-line shift when estimating the contribution from the OEC. As in the case of neutral red, this corresponds to an overestimate of the oscillatory contrast in the sequences that leads one to interpret the

1.1, 0.25, 1, 1.65 pattern (found here at pH 7) as a more contrasted 1, 0, 1, 2 pattern.

Before discussing the interpretation of our results, it may be useful to recall the theoretical treatment of noninteger proton stoichiometries as given by McPherson et al. (1988) and Maroti and Wraight (1988). One considers a protonatable group G in the vicinity of an electron carrier D. When D is oxidized to D^+, the potential experienced by G increases and its pK decreases accordingly. This results in a pH-dependent proton release which depends on the difference between the protonation degrees of G before the oxidation [controlled by the pK in the presence of D, pK(D)] and after the oxidation [controlled by the shifted p$K(D^+)$]. It is expressed by $\Delta H = 1/(1 + 10^{pH-pK(D)}) - 1/(1 + 10^{pH-pK(D^+)})$. The release is pH-dependent around the pK(D) and p$K(D^+)$ value and reaches a plateau of 1 only when the pK shift is sufficiently large. A useful guiding rule may be retained from this analysis. When the proton release *decreases* with increasing pH, the process is controlled by the prior protonation state of G in the presence of (reduced) D, and the variation occurs around pK(D). Conversely, when proton release *increases* with pH, the process is modulated around p$K(D^+)$. Now, in a more general way, when a charge appears on a redox carrier in a protein, it will influence a number of groups, and the resulting deprotonation will depend on the whole interplay of electrostatic interactions. It is worth noting that a single positive charge may trigger the release of more than one proton: in this case, the oxidation will result in a net charge *decrease* of the protein.

With this in mind, we may now proceed to analyze the results of Figure 4. Fom pH 5.5 to 8, we observed a continuous decrease of ϵ_0 from about 1.75 to 1, an increase of ϵ_1 from zero to 0.5 with a peak around pH 7.75, and a plateau close to 1 for ϵ_2.

The shape of the ϵ_0 curve may be accommodated by a superimposition of two processes, namely, a constant plateau at level 1 and a single group titration curve with pK around 6.05 (this value as well as the other pK's given in the following was estimated from a best fit of the data, corresponding to the curves drawn in the figure). This suggests that state S_1 is influencing electrostatically two groups. The first one, G_1, is fully protonated in the presence of S_0 and undergoes full deprotonation in the presence of S_1. Thus, for this group, p$K(S_0) \geq 9.5$ and p$K(S_1) \leq 4.5$, meaning a strong electrostatic interaction. The second group, G_2, is responsible for the observed *decrease* of the release with pH. Thus the pK involved must be the one occurring in the presence of the *reduced species*, S_0. The curve may be fitted by assuming for this group p$K(S_0) = 6.05$ and p$K(S_1) \leq 4.5$. The curve drawn in Figure 4 was computed using the upper limit (4.5) for the pK's of G_0 and G_1 in the presence of S_1: this accounts for the leveling off at low pH that better accommodates the pH 5.5 data point. Below pH 7.5, the $S_0 \rightarrow S_1$ transition causes the release of more than one proton: this means a negative change of the net charge, which in indeed consistent with the opposite direction of the electrochromic response (Figure 6) with respect to that occurring upon $S_1 \rightarrow S_2$.

According to the foregoing, both groups G_1 and G_2 are fully deprotonated in state S_1. The shape of the $S_1 \rightarrow S_2$ titration with a peak around 7.75 requires the introduction of (at least) one other group G_3, which deprotonates around pH 8.2 in the presence of S_1 or around pH 7.25 in the presence of S_2. Some comments may be added as to the finding of a pK around 8.2 in the presence of S_1. This pK must be introduced because of the decrease of the $S_1 \rightarrow S_2$ titration above pH 7.75. Although this is close to the alkaline limit of our experiments, the information indicating the presence of this pK resides in all four data points above pH 7, which would lie significantly below a titration curve involving only deprotonation of S_2. Furthermore, the experiment run in the presence of DCMU (Figure 5), which extends up to pH 8.25, gives an independent confirmation that a peak does occur around pH 7.75. Now, we have to account for the fact that this pK on state S_1 does not seem to modulate the $S_0 \rightarrow S_1$ curve. This suggests that the protonation state of G_3 is not significantly affected during the $S_0 \rightarrow S_1$ transition. It is rather natural to expect that such is the case above pH 7.25, where this transition is globally neutral (one proton released). Below this pH, however, the transition results in a negative net charge (more than one proton released), as corroborated by the direction of the electrochromic change: thus the pK of G_3 may be *more acid* in the presence of S_0. If it happens to be lower than 7.25, the $S_0 \rightarrow S_1$ titration would contain some uptake contribution on G_3, and the pK values given in Table I for G_2 and G_3 in state S_0 would be somewhat underestimated.

Table I: Summary of Various pK's Involved in Fitting of the Data of Figures 4 and 5

	S_0	S_1	S_2	S_3
G_1	≥9.5	≤4.5	≤4.5	≤4.5
G_2	6.05[a]	≤4.5	≤4.5	≤4.5
G_3	8.2[a]	8.2	7.25	7.25
G_4	≥9.5	≥9.5	≥9.5	≤3.5

[a] Possible uncertainty as discussed in the text.

Proton release during the $S_2 \rightarrow S_3$ transition remains close to 1, within experimental accuracy. This may be described in the present framework by assuming formally a group G_4, fully protonated in S_2 [p$K(S_2) \geq 9.5$] and fully deprotonated in S_3 [p$K(S_3) \leq 3.5$]. Again, it may be noticed that the pK found for G_3 in the presence of S_2 (around 7.25) causes no significant modulation of the $S_2 \rightarrow S_3$ titration. Thus, the net charge compensation maintained by the deprotonation of G_4 results in negligible potential change on G_3.

The final transition $S_3 \rightarrow S_4 \rightarrow S_0$ carries no further information since the proton release on this step is just the complement to 4 of the preceding ones. It expresses the balance between the final release of protons from water and the (pH-dependent) reprotonation of groups G_1–G_4.

The foregoing scheme is summarized in Table I, and its agreement with the data is illustrated in Figure 4 showing the curves computed with this set of pK's. It should be emphasized that the model we propose is by no means the only possible one, but the most parsimonious, that accounts for the data over the pH range investigated.

The change occurring on the first flash was not taken into account in the deconvolution of proton release sequences. As discussed elsewhere (Lavergne, 1991, 1987; Dekker et al., 1984), an additional contribution of "inactive centers" (Chylla et al., 1987; Graan & Ort, 1987) is present on the first flash in dark-adapted material. The offset found in the present experiments between the experimental value and that computed from the rest of the sequence seems however too large to arise from the ~25% inactive centers. Thus, an additional anomaly on protolytic reactions appears on the first flash. We observed (not shown) a marked dependence of this phenomenon on the presence of divalent cations. It may be noticed that the experiment of Figure 5 (with DCMU) gave similar results to those obtained from sequence deconvolution (first flash excluded). However, the elimination of the interfering phenomenon in this experiment is not necessarily an effect of DCMU (which would incriminate the acceptor side) but may alternatively be due to the use of preilluminated samples.

The titration of the electrochromic change caused by the successive transitions (Figure 6) shows a clear correlation with the proton release data. It should be stressed, however, that when the release process involves a pK shift caused by electrostatic influence of a redox center on a distinct protonatable group, the electric potential shift experienced by the pigment probe depends on the geometry of the system. For instance, if we call P the probe and imagine that it is aligned with the redox center D and a protonated group GH, then upon oxidation of D, causing deprotonation of GH, P will experience a negative or positive potential change, depending on whether the geometry is, respectively, D–GH–P or GH–D–P. Thus, in general, the magnitude and even direction of the electrochromic shift may differ from the overall net charge balance resulting from the oxidation/deprotonation process. In order to investigate such effects, the proton release curves from the fit of Figure 4 were replotted in Figure 6 with (arbitrary) normalization on the pH 6.5 data point of $S_1 \rightarrow S_2$. Within experimental accuracy, the electrochromic data turn out to be reasonably well fitted by these curves, provided a small vertical shift is given to the $S_0 \rightarrow S_1$ and $S_2 \rightarrow S_3$ titrations. In the latter case the offset is probably meaningless, since it may just express the contribution of the tail of the UV band associated with this transition to the wavelength difference used here. The spectrum shown in the right-hand part of Figure 6 does not establish unambiguously the presence of a significant electrochromic contribution on this transition. On the other hand, the upward offset of the electrochromic data with respect to the proton titration on $S_0 \rightarrow S_1$ (in the particular normalization adopted here) may be significant and may express a geometrical effect (e.g., group G_1 located closer to the probe than the other charge carriers involved). Nevertheless, the main result is an overall agreement between the electrochromic response and the electrostatic balance deduced from the proton release. This indicates that the probe is sufficiently remote from the charge carriers (redox centers and protonatable groups) to experience their collective action. It also suggests that the electrostatics of the system is primarily controlled by H^+ (or OH^-) movements, with little or no contribution of other ions (such as Cl^- or Ca^{2+}).

For simplicity, we have adopted so far an explanatory framework involving electrostatic interaction between redox centers and distinct protonatable groups. One should not exclude, however, the case when the redox center *itself* deprotonates when oxidized. This "chemical deprotonation" mechanism is, in a way, a limiting case of the "electrostatic deprotonation", when the D–G distance becomes small. Accordingly, one expects in this case a large value for the pK shift. Furthermore, since the molecular charge is conserved in this oxidation/deprotonation process, it should cause only minor (dipolar) electrostatic change on the environment. These features make it unlikely that a chemical deprotonation is involved in either the $S_0 \rightarrow S_1$ or $S_1 \rightarrow S_2$ transitions. Below pH 7.25, more than one proton is released upon the $S_0 \rightarrow S_1$ step. A chemical deprotonation involving two protons per electron would be rather exceptional, while, as alluded above, it is not unexpected in the electrostatic case when two groups are close enough to the redox center. In the case of group G_3 involved in the $S_1 \rightarrow S_2$ step, we found a $\Delta pK \approx 0.95$, which seems too small for a chemical deprotonation. We thus conclude that, in all likelihood, groups G_1–G_3 are subject to an electrostatic type of deprotonation, being distinct from the redox centers involved in the two first transitions. By contrast, there is no indication that the deprotonation on $S_2 \rightarrow S_3$ (group G_4) expresses the electrostatic mechanism rather than a chemical deprotonation. We found that a large pK shift ($\geq$6 units) was necessary to account for the flat titration curve on this transition. We also had to involve a large pK shift ($\geq$5 units) in the case of G_1, but noticed that the effect on G_2 was hardly compatible with a chemical deprotonation of G_1. The opposite situation seems to prevail on G_4 since the $S_2 \rightarrow S_3$ transition appears neutral for the, presumably close, G_3. Thus we believe the odds are rather in favor of a chemical deprotonation of G_4. The present picture, in which the two first transitions involve distinct redox centers and proton releasing groups, while a chemical mechanism occurs on the third transition, would agree with the view that a manganese oxidation occurs on both $S_0 \rightarrow S_1$ and $S_1 \rightarrow S_2$, whereas $S_2 \rightarrow S_3$ expresses oxidation of an amino acid residue (Boussac et al., 1991; Lavergne, 1991). It was suggested that the latter step could consist of formation of an OH adduct on an imidazole or indole ring, which would of course account for a deprotonation of the "chemical" type.

In earlier investigations concerning pH titrations of the donor side of PS II, two types of problems have been addressed: the rate of the $Y_Z\ P^+_{680} \rightarrow Y_Z^+\ P_{680}$ reaction (either in oxygen-evolving or in Tris-washed systems) and the rate of reactions between the S states and the auxiliary tyrosine Y_D. The latter problem, which is of more direct relevance to the present work, was recently investigated by Vass and Styring (1991), who reported a p$K \approx 5.9$ that was found to control the rate of the $S_0Y^+_D \rightarrow S_1Y_D$ reaction and, thus, was associated with state S_0. This pK is quite consistent with our p$K \approx 6.05$ on G_2 in the same state.

Considering the values given in Table I and leaving apart those given as upper or lower bounds, we have pK = 6.05 for G_2 and 8.2 for G_3 in the presence of S_0, which may reasonably be adopted as the "ground state" for the electrostatics of the system. It would be plausible to attribute G_2 to an histidine and G_3 to a cysteine. However, caution is required in such attributions, since large pK shifts are frequently occurring in proteins (Bashford & Karplus, 1990).

A drastically different proton release stoichiometry with respect to chloroplasts or BBY's has been reported by Lübbers and Junge (1990) and Wacker et al. (1990) in oxygen-evolving "core particles". In this material the pattern is nonoscillating with one proton released on each transition. This behavior is just what would happen if the system becomes unshielded so that many more protonatable groups in the vicinity of the OEC become accessible to the aqueous medium. If the pK spread of these groups is sufficiently large, any net charge change will be canceled through the electrostatically induced pK shifts (a process that may be compared with charge compensation by diffuse layers in the Debye–Hückel or Gouy–Chapman theories). While this nonspecific process is probably of little consequence on the mechanism of water oxidation, the oscillating pattern observed in the native system provides relevant information on this mechanism, such as, e.g., the "chemical" deprotonation that we proposed for the $S_2 \rightarrow S_3$ transition.

Registry No. H^+, 12408-02-5; H_2O, 7732-18-5.

References

Ausländer, W., & Junge, W. (1975) *FEBS Lett. 59*, 310–315.

Babcock, G. T. (1987) in *Photosynthesis: New Comprehensive Biochemistry* (Amesz, J., Ed.) Vol. 15, pp 125–158, Elsevier, Amsterdam.

Bashford, D., & Karplus, M. (1990) *Biochemistry 29*, 10219–10225.

Berthold, D. A., Babcock, G. T., & Yocum, C. F. (1981) *FEBS Lett. 134*, 231–234.

Boussac, A., Zimmermann, J. L., Rutherford, A. W., & Lavergne, J. (1991) *Nature 347*, 303-306.
Chylla, R., Garab, G., & Whithmarsh, J. (1987) in *Progress in Photosynthesis Research* (Biggins, J., Ed.) Vol. 2, pp 237-240, Martinus Nijhoff, Dordrecht.
Dekker, J. P., Van Gorkom, H. J., Wensink, J., & Ouwehand, L. (1984) *Biochim. Biophys. Acta 767*, 1-9.
Förster, V., & Junge, W. (1985) *Photochem. Photobiol. 41*, 183-190.
Fowler, C. F. (1977a) *Biochim. Biophys. Acta 462*, 414-421.
Fowler, C. F. (1977b) *Biochim. Biophys. Acta 459*, 351-363.
Fowler, C. F., & Kok, B. (1976) *Biochim. Biophys. Acta 423*, 510-523.
Ghanotakis, D. F., & Babcock, G. T. (1983) *FEBS Lett. 153*, 231-234.
Graan, T., & Ort, D. R. (1987) in *Progress in Photosynthesis Research* (Biggins, J., Ed.) Vol. 2, pp 241-244, Martinus Nijhoff, Dordrecht.
Jahns, P., Lavergne, J., Rappaport, F., & Junge, W. (1991) *Biochim. Biophys. Acta 1057*, 313-319.
Joliot, P., & Kok, B. (1975) in *Bioenergetics of Photosynthesis* (Govindjee, Ed.) pp 387-412, Academic Press.
Joliot, P., & Joliot, A. (1984) *Biochim. Biophys. Acta 765*, 210-218.
Joliot, P., Béal, D., & Frilley, B. (1980) *J. Chim. Phys. 77*, 209-216.
Lavergne, J. (1987) *Biochim. Biophys. Acta 894*, 91-107.
Lavergne, J. (1991) *Biochim. Biophys. Acta* (in press).
Lavergne, J., & Rappaport, F. (1990) in *Current Research in Photosynthesis* (Baltscheffsky, M., Ed.) Vol. 1, pp 873-876, Kluwer Academic Publishers, Dordrecht.
Lavorel, J. (1978) *J. Theor. Biol. 57*, 171-185.
Lübbers, K., & Junge, W. (1990) in *Current Research in Photosynthesis* (Baltscheffsky, M., Ed.) Vol. 1, pp 877-880, Kluwer Academic Publishers, Dordrecht.
Maroti, P., & Wraight, C. A. (1988) *Biochim. Biophys. Acta 934*, 329-347.
McPherson, P. H., Okamura, M. Y., & Feher, G. (1988) *Biochim. Biophys. Acta 934*, 348-368.
Meyer, B., Schlodder, E., Dekker, J. P., & Witt, H. T. (1989) *Biochim. Biophys. Acta 974*, 36-43.
Petrouleas, V., & Diner, B. (1986) *Biochim. Biophys. Acta 849*, 264-275.
Polle, A., & Junge, W. (1986) *Biochim. Biophys. Acta 848*, 257-264.
Rutherford, A. W. (1989) *Trends Biochem. Sci. 14*, 227-232.
Saphon, S., & Crofts, A. R. (1977) *Z. Naturforsch. 32C*, 617-626.
Saygin, O., & Witt, H. T. (1985) *FEBS Lett. 178*, 224-226.
Vass, I., & Styring, S. (1991) *Biochemistry 30*, 830-839.
Velthuys, B. R. (1988) *Biochim. Biophys. Acta 933*, 249-257.
Wacker, U., Haag, E., & Renger, G. (1990) in *Current Research in Photosynthesis* (Baltscheffsky, M., Ed.) Vol. 1, pp 869-872, Kluwer Academic Publishers, Dordrecht.

Differences in Thermal Stability between Reduced and Oxidized Cytochrome b_{562} from *Escherichia coli*†

Mark T. Fisher*
Laboratory of Biochemistry, National Heart, Lung and Blood Institute, National Institutes of Health, Bethesda, Maryland 20892

Received May 21, 1991; Revised Manuscript Received July 29, 1991

ABSTRACT: The thermal stabilities of ferri- and ferrocytochrome b_{562} were examined. Thermally induced spectral changes, monitored by absorption and second-derivative spectroscopies, followed the dissociation of the heme moiety and the increased solvation of tyrosine residue(s) located in close proximity to the heme binding site. All observed thermal transitions were independent of the rate of temperature increase (0.5–2 °C/min), and the denatured protein exhibited partial to near-complete reversibility upon return to ambient temperature. The extent of renaturation of cytochrome b_{562} is dependent on the amount of time the unfolded conformer is exposed to temperatures above the transition temperature, T_m. All thermally induced spectra changes fit a simple two-state model, and the thermal transition was assumed to be reversible. The thermal transition for ferrocytochrome b_{562} yielded T_m and van't Hoff enthalpy (ΔH_{vH}) values of 81.0 °C and 137 kcal/mol, respectively. In contrast, T_m and ΔH_{vH} values obtained for the ferricytochrome were 66.7 °C and 110 kcal/mol, respectively. The estimated increase in the stabilization free energy at the T_m of ferricytochrome b_{562} following the one-electron reduction to the ferrous form, where $\Delta\Delta G = \Delta T_m \Delta S_m$ [ΔS_m = 324 cal/(K·mol), ΔT_m = 14.3 °C] [Becktel, W. J., & Schellman, J. A. (1987) *Biopolymers 26*, 1859-1877], is 4.6 kcal/mol.

Cytochrome b_{562} from *Escherichia coli* is a small (M_r 12000) water-soluble heme protein and is localized in the periplasmic space. This cytochrome contains an N-terminal leader sequence which is subsequently cleaved during or after transport through the inner periplasmic membrane (Nikkila, 1987). Although its functional role in *E. coli* is unknown, cytochrome b_{562} from *Acinetobacter calcoaceticus* has been proposed to function as an electron-transfer shuttle between the quinoprotein glucose dehydrogenase (+50 mV), localized in the periplasm, and ubiquinone (Doktor et al., 1988).

The structure of the *E. coli* cytochrome has been defined by X-ray crystallography to a resolution of 2.5 Å (Mathews et al., 1979). The protein folds in an antiparallel α-helical

† Preliminary experiments, performed in Dr. S. G. Sligar's laboratory, were supported by NIH Grants GM 33775 and GM 31756.
* Address correspondence to this author at NHLBI/NIH, Building 3, Room 207, Bethesda, MD 20892.